T.S.M.H Medical Nursing Journal

Structure, function and mechanical properties of selected biological materials

P.-Y. Chen[1], A.Y.M. Lin[1], Y.-S. Lin[2], M.A. Meyers[1,2] and J. McKittrick[1,2]
[1]Materials Science and Engineering Program, [2]Dept. of Mechanical and Aerospace Engineering, UC San Diego, La Jolla, CA 92037-0411

Abstract

Mineralized biological tissues offer insights into how nature has evolved these components to optimize multifunctional purposes. These mineral constituents are weak by themselves, but interact with the organic matrix to produce materials with unexpected mechanical properties. The hierarchical structure of these materials is at the crux of this enhancement. Microstructural features such as organized, layered organic/inorganic structure, and the presence of porous and fibrous elements are common in many biological components. The organic and inorganic portions interact at the molecular and micro-levels synergistically to enhance the mechanical function. In this paper, we report on recent progress on studies of the abalone shell, crab exoskeletons, antlers, tusks, teeth.

Keywords: mechanical properties, biological materials, biomimetics, abalone, crab, horseshoe crab, antler, hippo teeth, warthog tusk, great white shark teeth, piranha teeth, dogfish teeth

INTRODUCTION

The study of biological materials has received increasing interest in recent years due to the often extraordinary mechanical properties and unusual structures these materials possess. For example, the nacre of the abalone shell has been reported to have a work of fracture 3000x over that of the mineral constituent (Jackson et al. 1988a). The compressive stress of a shark tooth bite is measured as high as 600 MPa (Snodgrass and Gilbert, 1967), even though this exceeds the compressive strength of the individual mineralized portions of the tooth (Craig et al. 1958, 1961). Spider silk is reported to have a tensile strength similar to high-grade steel (Vollrath et al. 2001) and the gecko foot has been found to have exceptional der Waals forces (Autumn et al. 2000, Arzt et al. 2003).Biological structural materials fulfill numerous purposes.

Received：Aug, 11, 2010 **Accepted： Sep, 23, 2010**
Communication author: Po-Yu Chen
Address：9500 Gilman Drive, La Jolla, CA 92093-0411
Telephone：1-858-534-6091 Fax：1-858-534-5698 E-mail：pochen@ucsd.edu
Transdlator： Pao-Sheng Chen,National Tsing Hua University, Department of Materails Science and Engineering
Proofreader： Jenq-Gong Duh, National Tsing Hua University, Department of Materails Science and Engineering Professor
Telephone：03-5712686 Fax：03-5712686 E-mail：jgd@mx.nthu.edu.tw

Antlers must flex without breaking and be impact resistant, mollusk shells must be able to sustain loads (wave and predator) without fracture, bones and teeth must maintain large compressive forces without buckling and/or cracking and plants must bend without tearing.

Many biological systems have mechanical properties that are far beyond those that can be achieved using the same synthetic materials (Vincent, 1991; Srinivasan et al., 1991). This is a surprising fact, if we consider that the basic polymers and minerals used in natural systems are quite weak. This limited strength of the components is the result of the ambient temperature, aqueous environment processing, as well as of the limited availability of elements (primarily C, N, Ca, H, O, Si). Biological organisms produce composites that are organized in terms of composition and structure, containing both inorganic and organic components in complex structures. They are hierarchically organized from the molecular to the macro (structural) level. The emerging field of the study of biological materials offers new opportunities to materials scientists to do what they do best: solve complex multidisciplinary scientific problems.

Hard biological materials are composites of an inorganic oxide phase with a biopolymer, created in a process called biomineralization. Biomineralized hydroxyapatite ($Ca_{10}(PO_4)_6(OH)_2$, the main mineral component bone, teeth and antlers), calcium carbonate ($CaCO_3$ in the form of calcite or aragonite), the main component of seashells, bird eggs, crustaceans and coral) and amorphous silica ($SiO_2(H_2O)_n$, the main mineral content of sponge spicules and diatoms) have been the primary materials examined.

The study of hard biological materials such as seashells, antler, teeth and bone have yielded fascinating insights into how these inorganic/organic materials adjust their microstructure and growth conditions to provide superior structural properties. A property map showing Young's modulus as a function of density is shown in Figure 1. Biomineralized composites such as the mollusk shell, coral, teeth, for example, are very lightweight but have a high elastic modulus. The densities of biological materials are generally less than 3 g/cm^3. These materials have an integrated, hierarchical structure with an increasing complexity of the macroconstituents as the dimension becomes smaller. The macro shape has been optimized for external influences such as protection and fighting and the nanoscale displays an intricate interaction between the mineral and organic components. This interaction, which has components of strong chemical and mechanical adherence, is maintained throughout the various length scales. It has been shown by Ji et al. (2004) and Gao et al. (2003) that the scale of the components is important for the optimized performance. Using the Griffith criterion for brittle fracture, the stress (σ) required to activate a flaw of size 2a is:

$$\sigma = \frac{K_c}{\sqrt{\pi a}}$$

where K_c is the toughness of the brittle component. The fracture toughness is ~ 1 MPa√m for aragonite (Meyers et al. (2007) and ~ 1.2 MPa√m for hydroxyapatite (van der Lang et al. (2002)). From Figure 1, the elastic modulus of aragonite and hydroxyapatite is ~ 100 GPa. Estimating that the theoretical strength of the material is E/10, this strength is reached for a~ 25 nm. This is part of the reason why the brittle component scale is in the nanometer range.

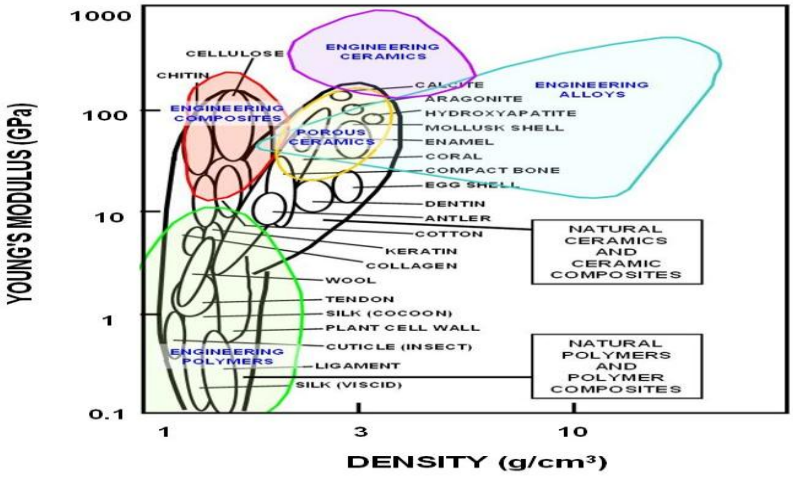

Figure 1. Young's modulus as a function of density for various biological materials, overlaid on a map indicating regions of synthetic materials (Adapted from Ashby (1989) and Wegst and Ashby (2004)).

One striking similarity between mineralized tissues of various taxa is the presence of organized layered structures of soft and hard material. The mineralized phase provides strengthening and the organic phase provides toughness. This is observed in seashells and to some extent in compact bone. The interaction of the mineralized and organic components produces a synergistic effect that enhances mechanical properties. Another similarity is the presence of porous (foam) material in taxa that are ambulatory, as displayed in bones, antlers, arthropod exoskeletons and teeth. The porous material provides a lightweight framework and increases the stiffness of the biological component. Fibers are also preponderant in biological materials. Bones, teeth, crab exoskeletons and antler all have some fibrous component. Anisotropy of the fibers plays a major role in determining the mechanical properties of these components.

Analysis of laminates, porous and fibrous structures are at the heart of understanding the mechanical properties of biological materials. In this paper, we report recent progress on the structure, function and mechanical properties of the abalone shell, crab exoskeletons, antler, teeth and tusks.

Abalone shell

The abalone shell (*Haliotis rufescens)* has two layers: an outer prismatic layer (rhombohedral calcite) and an inner nacreous layer (orthorhombic aragonite) as observed by Nakahara et al. (1982). Figure 2(a) shows a shell with its nacreous (internal) surface exposed. The nacreous portion is composed of mesolayers of ~ 0.3 mm thick, separated by organic layers embedded with calcium carbonate (Meyers et al. 2008). These mesolayers are thought to be the result of growth bands and are visible in the optical micrograph of Figure 2(b). Aragonitic $CaCO_3$ constitutes the inorganic component of the nacreous ceramic/organic composite (95 wt-% ceramic, 5 wt-% organic material). This composite is comprised of stacked platelets (~0.5 μm thick), arranged in a 'brick-and-mortar' microstructure with an organic matrix (20-50 nm thick) interlayer that is traditionally considered as serving as glue between the single platelets (Figure 2(c)). As a result of this highly ordered hierarchical structure nacre exhibits excellent mechanical properties. Details of the structure and growth can be found in our work (Menig et al. 2000; Lin and Meyers, 2005; Lin et al. 2006, 2007; Meyers et al. 2008) and others (Watanabe and Wilber, 1960; Wada, 1964; Towe and Hamilton, 1968; Bevelander and Nakahara, 1970; Erben, 1972; Sarikaya and Aksay, 1992; Fritz et al., 1994; Manne et al., 1994; Falini et al. 1996; Zaremba et al., 1996; Schäffer et al., 1997; Addadi et al., 2006).

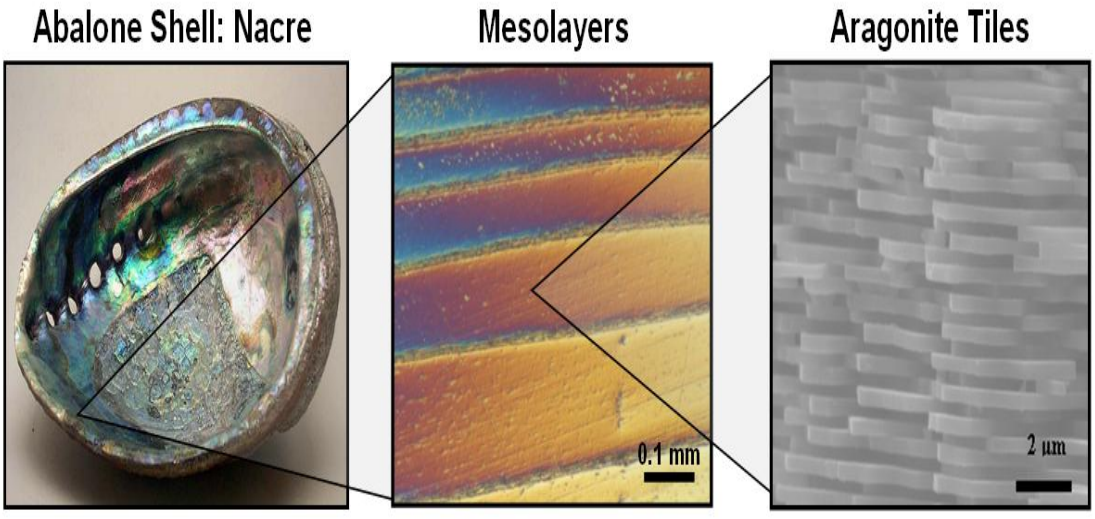

Figure 2. Hierarchical structure of abalone shell. (Abalone was harvested from the abalone tank located at the Scripps Institute of Oceanography).

Figure 3 summarizes the strength of nacre with respect to various loading directions. The unique strength anisotropy perpendicular to the layers (5 MPa vs. 540 MPa) is remarkable (Jackson et al. 1988b; Meyers et al. 2008).

Another marked characteristic is the greateter compressive strength when loading is applied perpendicular rather then parallel to the tiles. This is due to the phenomena of axial splitting and microbuckling (kinking) when loading is applied parallel to the tiles. The relatively small difference in tensile and compressive strength (170 MPa vs. 230 MPa (Menig et al., 2000)) in this direction of loading is directly related to the high toughness, possibly attributed to the existence of inter-tile mineral bridges in combination to the organic "glue". These mineral bridges exist as the continuation of a single crystal between consecutive layers of aragonite tiles.

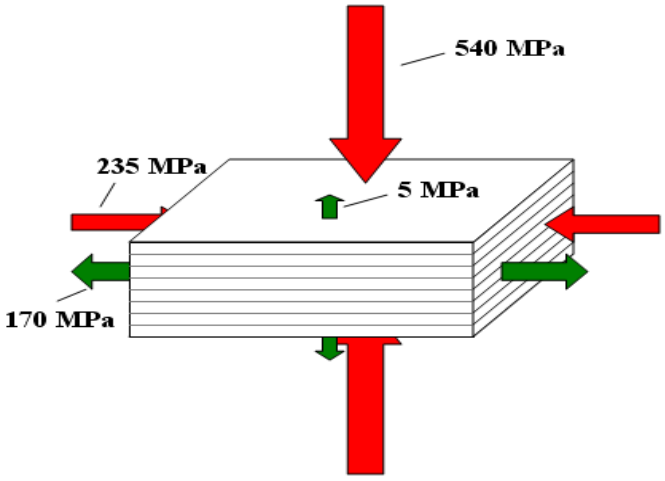

Figure 3. Compressive strength and ultimate tensile strength of nacre with respect to loading direction.

Figure 4 is a schematic showing the failure mechanisms for the different load applications and directions. Compression perpendicular to the surface of the shell yields the highest value, and failure occurs in an axial splitting mode. Compression parallel to the shell surface, on the other hand, reveals a fracture mode akin to plastic microbuckling (not always, but on a significant fraction of cases). This has been analyzed in detail by Menig et al. (2000). Failure in tension when the loading direction is parallel to the shell surface occurs by sliding of the tiles, so that this is relatively brittle fracture. Thus, the shear strength of the organic inter-tile layer is about the same (or higher) than the

tensile strength of the tiles, and failure occurs by inter-tile shear. For tensile loading perpendicular to the shell surface, the primary mechanisms seem to be fracture of the inter-tile bridges and extension of the organic layer gluing the adjacent layers.

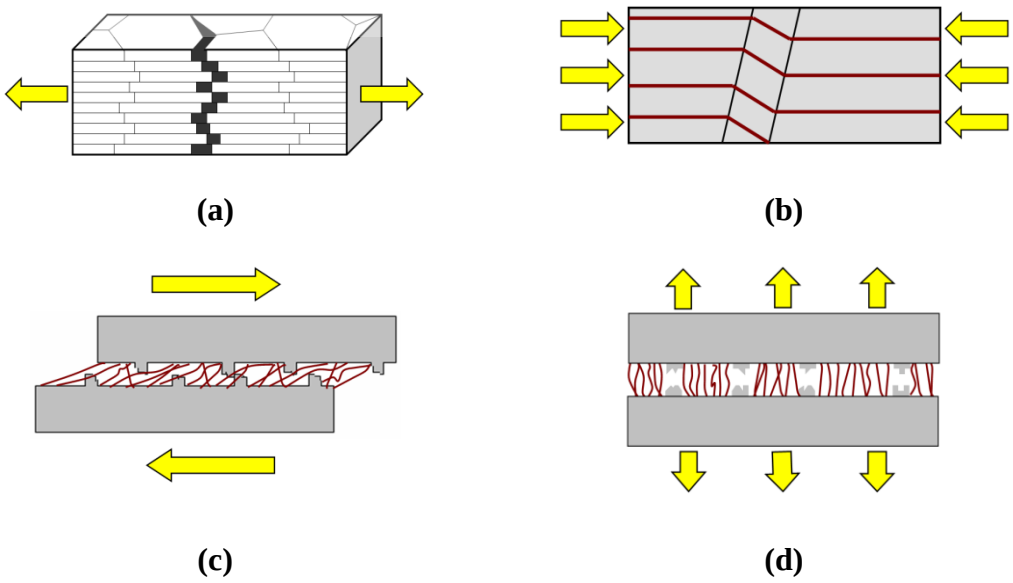

Figure 4. Failure mechanisms of abalone shells in different loading conditions: (a) Tension parallel to shell surface (b) compression parallel to shell surface (c) shear parallel to shell surface (b) tension perpendicular to shell surface.

Inter-tile mineral artifacts have been observed through transmission electron microscopy (TEM) as can be seen in Figure 5.

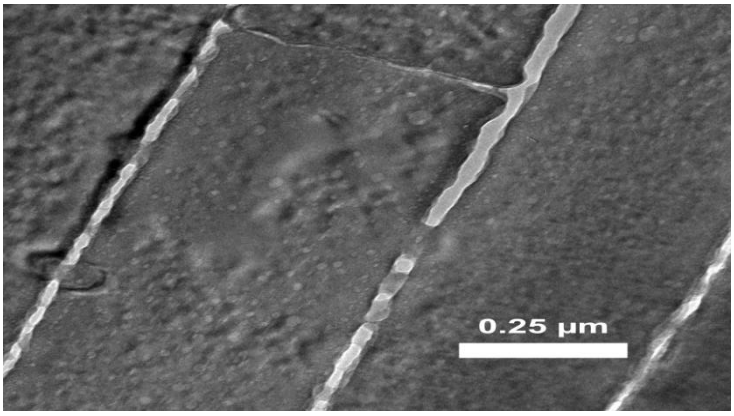

Figure 5. Transmission electron micrograph of nacre crossection showing mineral bridges between tile interfaces.

To prove that a mineral connection exists, selected area diffraction patterns were obtained for consecutive layers of tiles. Each subsequent tile showed identical crystal orientation, indicating single crystal continuity only possible through a mineral connection. These have been presented in Figures 6(a) and (b) and are in agreement with results by Feng et al. (1999) who also showed high degree of crystallographic texture characterized by a nearly perfect "c-axis" alignment normal to the plane of the tiles through selected area diffraction patterns. The observed mineral bridges are believed to grow as consecutive layers of tiles are formed and mediated through a series of porous organic membranes. This has been well described by Cartwright et al. (2007). Recent findings suggest that they play a critical role in both the growth and the mechanical strengthening of the composite (Lin et al. 2007; Meyers et al. 2008). The organic matrix was once thought to provide the primary interfacial toughening mechanisms. By observing the large ratio of compressive to tensile strength when loading is perpendicular to the tiles (Figure 3), one can begin to estimate the tensile strength of an individual mineral bridge (Meyers et al. 2008). Although there are a high number of bridges per tile (a density of approximately 2.25/μm^2 per tile), the total area along which a load can be applied in tension is still a fraction of the composite area. Thus a relatively low strength (5 MPa) is observed in this loading direction. Song et al. (2002) were among the first to identify these bridges and to estimate quantitatively their number. Barthelat et al. (2006) and Meyers et al. (2008) confirmed their presence.

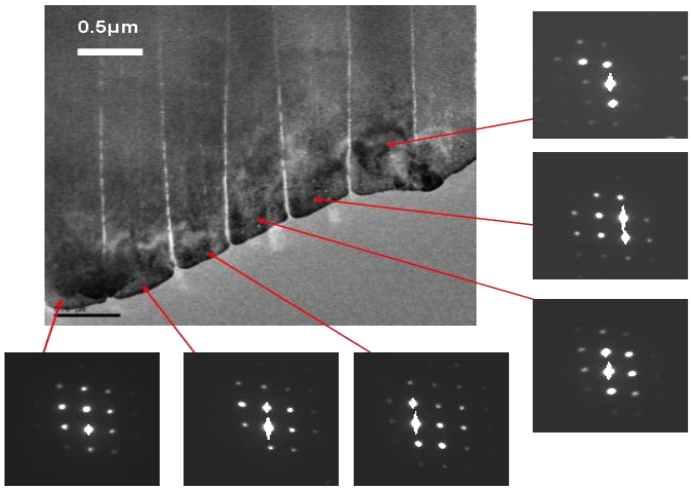

(a)

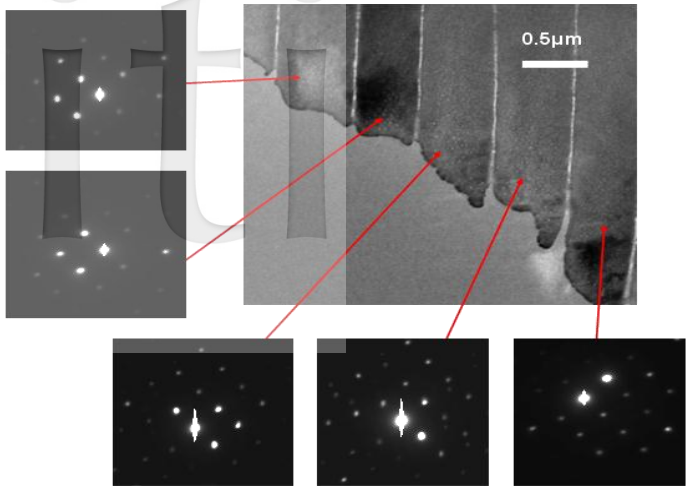

(b)

Figure 6. Two samples of abalone nacre (a) and (b) characterized through transmission electron microscopy. Consistent crystal orientation is observed through selected area diffraction of consecutive layers of aragonite tiles indicating a single crystal structure through several layers.

Crab exoskeleton

The arthropod exoskeleton is a natural composite which is multifunctional, hierarchically structured, and highly anisotropic in mechanical properties. Exoskeletons from two species, sheep crab (*Loxorhynchus grandis*) and horseshoe crab (*Limulus polyphemus*), have been investigated by our group. The arthropod exoskeleton is multifunctional: it supports the body, resists mechanical loads, and provides environmental protection (Vincent, 1991, 2002). The exoskeleton comprises three main layers, epicuticle, exocuticle, and endocuticle. The outermost epicuticle is a thin waxy layer, which acts as waterproofing barrier. Beneath the epicuticle is the exocuticle (outer) and endocuticle (inner), the main structural component, which is primarily designed to resist mechanical loads. There is a high density of pore canals containing tubules penetrating through the exoskeleton in the direction normal to the surface. These tubules play an important role in the transport of mineral ions and nutrition during the formation of the new exoskeleton after the molting.

The arthropod exoskeleton consists mainly of chitin and protein. In crustaceans (e.g. crabs and lobsters), there is a high degree of mineralization, typically $CaCO_3$ in the form of calcite. Figure 7(a) shows the hierarchical structure of a sheep crab (*Loxorhynchus grandis*) exoskeleton. At the molecular

level, chitin chains form fibrils of 3 nm in diameter and 300 nm in length. The fibrils are wrapped with proteins and assemble into fibers of about 60 nm in diameter. These fibers further assemble into bundles. The bundles form horizontal planes stacked in a helicoidal fashion, creating a twisted plywood structure. A complete 180° rotation is referred to as a Bouligand layer (Bouligand, 1972; Giraud-Guille, 1984). The Bouligand layer corresponds to the layers in exocuticle and endocuticle. Figure 7(b) shows the hierarchical structure of horseshoe crab (*Limulus polyphemus*) exoskeleton. The horseshoe crab is a living fossil, which has existed for more than 200 million years.

Horseshoe crabs are genetically more similar to scorpions and spiders than to other crabs. The exoskeleton of horseshoe crabs is a sandwich composite consisting of three layers: an exterior shell, an intermediate layer, and an interior core. The exterior shell of horseshoe crab is similar to crab exoskeletons with no mineral presence. Beneath the exterior shell is an intermediate layer consisting of vertical laminate about 2-3 μm wide that connects the exterior shell to the interior core. The interior core has an open-cell foam structure and is hollow in the middle. The cellular network is akin to the interior structure of toucan and hornbill beaks, as described in the below section.

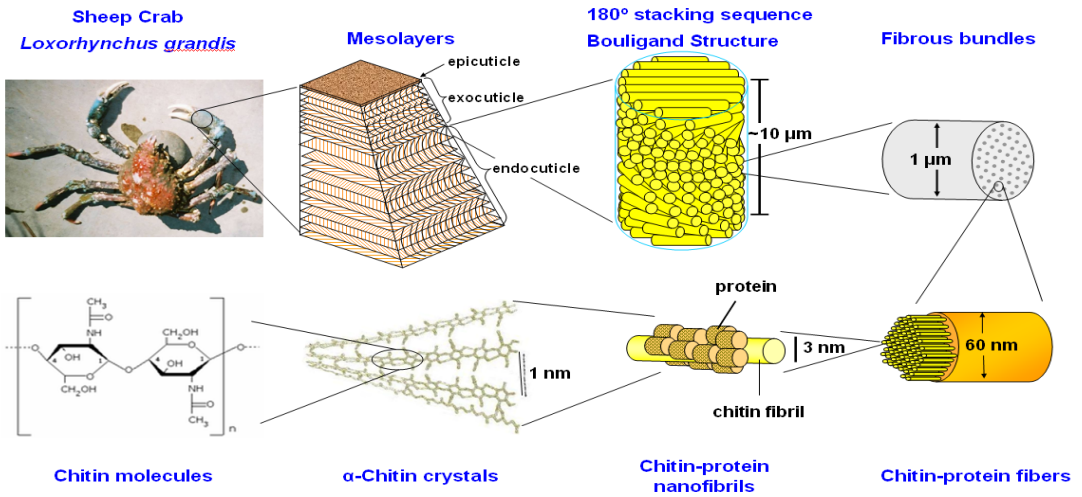

(a)

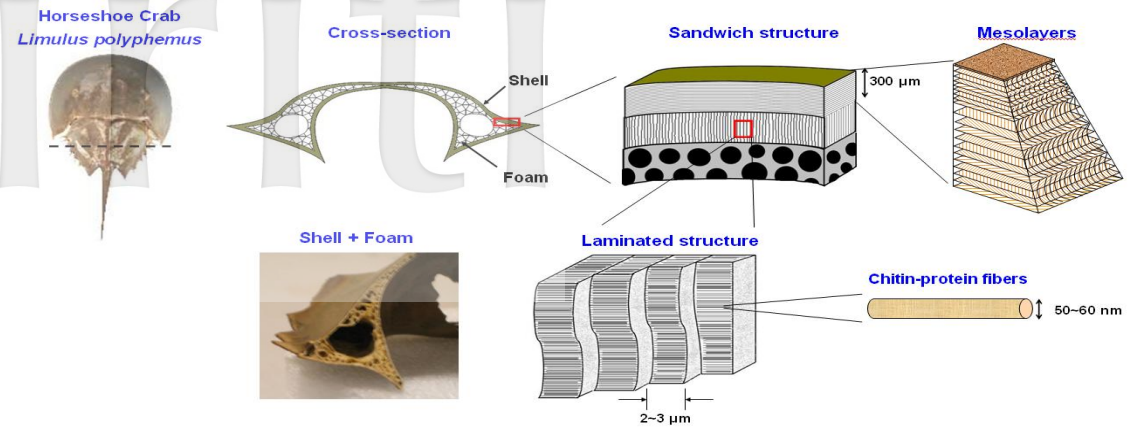

(b)

Figure 7. Hierarchical structure of (a) sheep crab (*Loxorhynchus grandis*), and (b) horseshoe crab exoskeletons. (sheep crabs were obtained locally from a fish market, a horseshoe crab was collected on a beach in Long Island, NY.)

Figure 8(a) is a scanning electron microscope (SEM) micrograph showing the Bouligand structure (brace) of sheep crab exoskeleton. In the normal direction, there are ribbon-like tubules (arrows) going through the layers. The width of a single tubule is about 1 µm and the thickness is about 0.2 µm. Figure 8(b) shows the exterior shell and intermediate layer of the horseshoe crab exoskeleton. The exterior shell has layered structure, which is akin to crab exoskeletons consisting epicuticle, exocuticle, and endocuticle. The intermediate layer is composed of vertically oriented laminate ~ 2-3 µm thick.

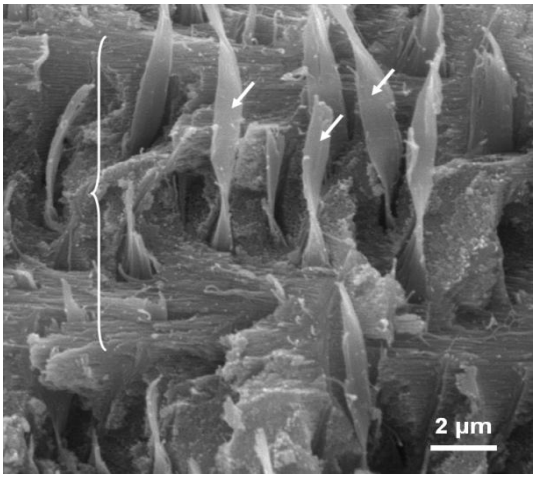

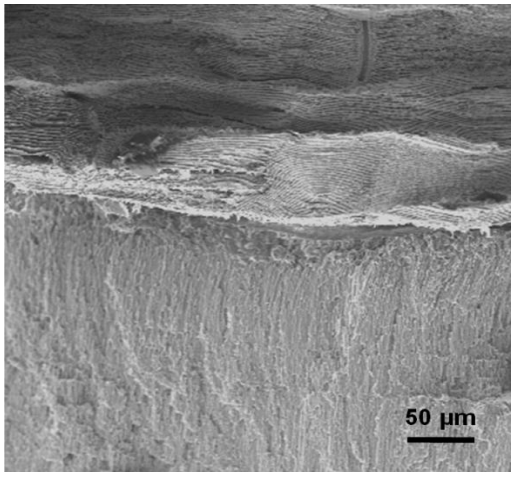

(a) **(b)**

Figure 8. SEM micrographs showing (a) the Bouligand structure of the sheep crab exoskeleton. (Brace: 180° rotation of Bouligand structure. Arrows: ribbon-shaped pore canal tubules) (b) the external shell and intermediate laminated layers of horseshoe crab exoskeletons.

The mechanical properties of arthropod exoskeleton are highly anisotropic. Tensile tests were performed on sheep crab exoskeletons in two different directions: longitudinal direction (y-direction) and direction normal to the surface (z-direction) (Chen et al. 2007). For the walking legs, in the y-direction, the stress-strain curve is linear and fracture occurs at 12.5 ± 2.3 MPa and 1.7 ± 0.3% strain. The flat fracture surface corresponds to brittle failure. In the z-direction, a non-linear plastic deformation is observed and the ultimate tensile strength reaches 18.8 ± 1.5 MPa and 4.7 ± 1.2% strain. There is a high density of tubules ruptured in tension and necking can be observed. Tubules act as the ductile component that helps to stitch the brittle bundles arranged in Bouligand pattern and enhance toughness**.**

Hardness tests were conducted on the claw and walking leg of sheep crab from the surface through the thickness of exoskeleton. The results show that the exocuticle is much harder than endocuticle. A discontinuity of hardness values across the interface between the exocuticle and the endocuticle is observed. The hardness values are 948 ± 108 MPa (claw) and 238 ± 35 MPa (walking leg) in the exocuticle region (~200 μm thick) and drop to a much lower value, ranging 440-540 MPa (claw) and 130-142 MPa (walking leg) in the endocuticle (~2.5 mm thick). This is due to the higher mineral content and the more densely packed structure in the exocuticle.

The hardness values of the claw are about 3-4 times higher than those of the walking legs.

This correlates with the higher mineral content in claw (78.5 wt% ash) compared to the walking leg (63.5 wt% ash). The hardness values measured in this work are higher than those of the American lobster claw (130-270 MPa in exocuticle and 30-55 MPa in endocuticle) (Raabe et al., 2005). This may also relate to the higher mineral content in sheep crab compared with the American lobster, which has an ash content of 63.6 ± 4.3 % of dry weight. Such design (hard, thin layer on the surface) is widely used in nature. For example, teeth and tusks are comprised of a hard external hard enamel and internal tough dentine.

Antlers

Antlers offer an interesting area of study because they are one of the most impact resistant, energy absorbent of all biomineralized materials. Antlers are bony protuberances that form on the heads on animals from the Cervidae family (deer). The Cervidae family includes deer, moose, American elk (wapiti) and reindeer (caribou). Antlers are one of the fastest growing organs in the animal kingdom, growing as much as 14 kg in 6 month, with a peak growth rate of up to 2-4 cm/day (Goss, 1983). The antler is the only mammalian bone that is capable of regeneration, offering unique insights into bone growth. Antlers are deciduous and are cast off (dropped) at the end of the rut (Sept. – Nov.). Antlers have two primary functions: they serve as visual signs of social rank within bachelor groups (Geist, 1966; Henshaw, 1971; Lincoln, 1972, Clutton-Brock, 1982) and are used in combat, both as a shield and as a weapon (Geist, 1966). During the rut, male deer fight for control of harems, which involves charging, butting heads and interlocking antlers. The antlers have been designed to undergo high impact loading and large bending moments without fracture. The unusual strength of antlers is attested by the very few observations of antler breakage during fighting in large groups of caribou and moose (Henshaw, 1971). Antlers have a composition and structure similar to other mammalian long bones, but there are distinct differences. Bones are load bearing and contain essential interior fluids (blood, marrow, etc.). Bones produce vital cells necessary for the body whereas antlers remove fluids and minerals from the body in order to grow. Antler growth (antlerogenesis) necessitates a large amount of calcium and phosphorus in a short period of time. Red deer (*Cervus elaphus*, a European deer almost identical to the American elk) antlers require ~ 100 gm/day of bone material in comparison to the growing fawn skeleton that take ~ 34 gm/day (Chapman 1975).

This quantity of minerals cannot be obtained through food sources alone and has been shown to originate from the skeleton of the animal (Meister, 1956; Chapman 1975; Goss, 1983; Muir et al. 1987; Harvey and Bradbury, 1991)

The long bones of the legs and the ribs are the richest source of these minerals, and these bones are found to decrease in density as the antlers increase in size. Bone resorption occurs along side bone remodeling during antlerogenesis. Another difference between antlers and other bones is the mineral content. Antlers have ~ 50 wt.% mineral content whereas bones are between 60 - 70 wt.% (Currey, 1979).

Figure 9 shows the hierarchical structure of antlers. Antlers contain a core of trabecular (cancellous) bone surrounded by compact bone that runs longitudinally through the main beam of the antler and the prongs. The trabecular bone is anisotropic, with somewhat aligned channels directed parallel to the long axis of the antler beam. Compact bone surrounds this core, consisting of osteons (Haversian system) that have a laminated structure of concentric rings extending from the main channel (blood vessel). The concentric rings contain aligned collagen fibrils that have the mineral, hydroxyapatite, dispersed on or between the fibrils. The alignment of the collagen fibrils changes direction between the laminates.

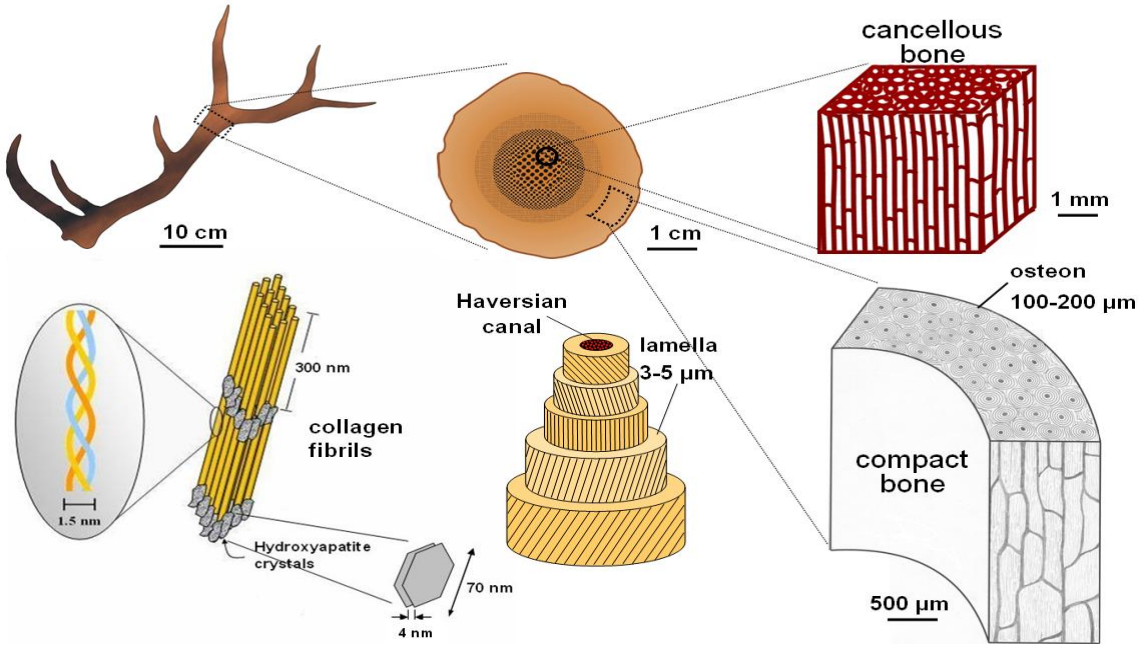

Figure 9. Hierarchical structure of antlers. Antlers are composed of primarily compact bone as the outer layer and trabecular (cancallous or spongy) bone in the interior. The compact bone consists of osteons, which supply blood to the growing antler through the Haversian canals. (Antlers and tusks were purchased from Into the Wilderness Trading Company, Pinedale, WY.)

The antlers from the American elk (*Cervus Canadensis*) were examined in this study. Figure 10(a) shows a photograph of a cross-section of piece taken from the long beam of the antler. The thin, outer most layer is the subvelvet zone, below which is the compact bone. There is a transition region between compact bone and the porous, spongy bone (trabecular bone) in the interior (Currey, 1988). This is to be contrasted with the long bones of mammals, which have a hollow interior (except at the head of the bone, where cancellous bone is found). The inset shows the osteons in the compact bone, which has the same configuration of other mammalian bones.

Figure 10(b) shows a computer tomography (CT) scan of the longitudinal cross-section demineralized portion of the antler. The elongated channels in the trabecular bone can be seen.

Some mechanical testing has been performed on antlers. Currey first performed experiments on bones and antlers taken from various species (Currey, 1979, 1988, 1989, 1990) and found that the elastic modulus increased and toughness decreased with increasing mineral content.

Blob et al. tested white tailed deer (Blob and LaBarbera, 2001) (*Odocoileus virginianus*) and moose (*Alces alces*) (Blob and Snelgrove, 2006) antlers and found no correlation of the elastic modulus as a function of the position along the antler, suggesting that other mechanical properties may not be influenced by the location. Moose antlers had a higher elastic modulus (11.6 GPa) compared to the white-tailed deer (6.8 GPa). The difference was attributed to the different fighting behavior between moose and the white-tailed deer as a consequence (or a predicator) of the different antler structure. Moose have large palmate antlers, with small prongs surrounding it. Deer have a long antler beam with prongs extending from this central beam. As a consequence, fighting moose cannot interlock their antlers and are thus subjected to higher bending moments. The elastic modulus of the elk antler is ~ 7.5 GPa, which is smaller than for moose and larger than for white-tailed deer. As expected, it is nearly identical to that of red deer (7.4 GPa, Currey 1979).

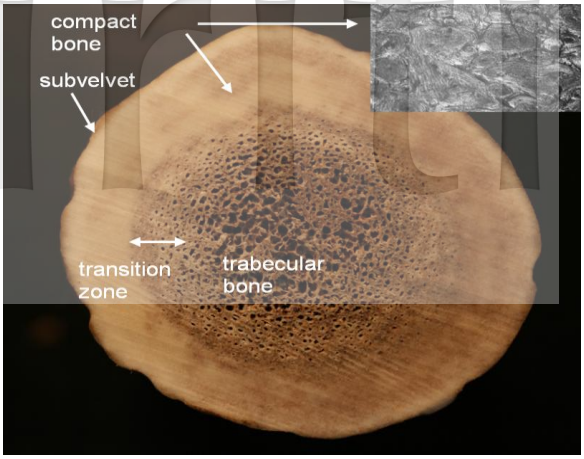

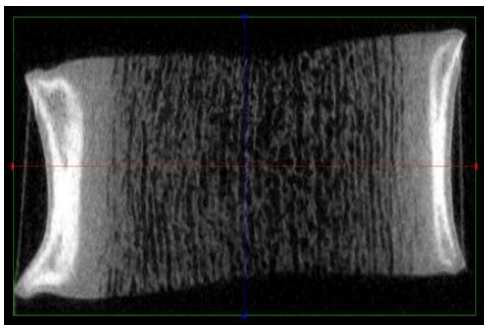

(a) **(b)**

Figure 10. (a) Cross-section through the main beam of an American elk. The thin outer surface is the subvelvet zone followed by compact and trabecular bone. A transition zone separates the compact and trabecular regions. Inset is an SEM micrograph of the compact bone showing the osteon. (b) Computer tomography scan of a demineralized antler. (Antlers and tusks were purchased from Into the Wilderness Trading Company, Pinedale, WY.)

Figure 11 shows a Weibull plot of the dry tensile strength in the longitudinal and transverse direction of compact bone along the main beam of the elk. The plot shows that the strengths can be fit with Weibull statistics. The strength in the transverse direction (N = 9) has an average failure strength of 20.3 ± 6.0 MPa compared with the longitudinal strength of 115.4 ± 16.6 MPa (N = 7). The strength in the longitudinal direction is lower than the antler strength of the spotted deer (*Axis axis*) of 188 ± 12 MPa (Rajaram and Ramanathan, 1982), and the red deer (158 MPa) and larger than reindeer (*Rangifer tarandus*, 95 MPa) (Currey, 1990). For comparison, the dry longitudinal tensile strength of the compact bone of a cow femur is 148 MPa (Currey, 1990). These comparable values indicate the similarity of structure of compact bone in long bones and in antlers. The Weibull modulus in the transverse direction has a smaller Weibull modulus, illustrating larger scatter in the data. This is a consequence of the anisotropic orientation of mineralized collagen fibers. The collagen fibers are oriented roughly along the longitudinal axis, preventing cracks from propagation. In

the transverse direction, cracks can more easily propagate through the interstice between neighboring lamellae and the value of tensile strength in the transverse direction depends on the presence of surface cracks.

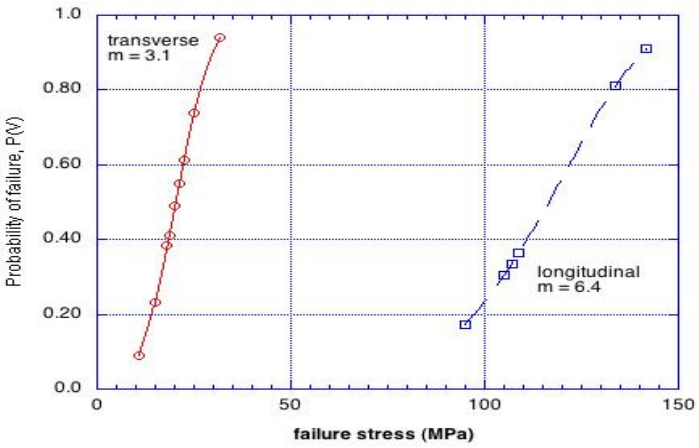

Figure 11. Weibull plot of the dry transverse and longitudinal strengths of the elk antler. m = Weibull modulus.

Tusks and teeth

Teeth are the most mineralized component of vertebrate animals and are composed of four parts. The outer layer is enamel, with a mineral content of 96% hydroxyapatite in the form of woven rods. Below the enamel is dentin containing 30% type-I collagen, 25% fluid and 45% nanocrystalline carbonated apatite (Imbeni et al. 2003; Meyers et al. 2007). Cementum, covering the root of the tooth, has ~ 65% hydroxyapatite, 23% type-I collagen and 12% water. Finally, dental pulp is at the center of the tooth is highly vascularized with nerves, cells and some type-I collagen. Depending on the diet of the animal, teeth are optimized for chewing (herbivores) or biting and tearing (carnivores). A tusk is an extremely long mammalian tooth that protrudes from of the mouth. Tusk-bearing mammals include the

walrus, elephant, warthog and narwhal. Large teeth and tusks are often used interchangably to describe ivory.

Hippopotamus (*Hippopotamus amphibious*) have very large curved canines in front, slightly smaller incisors just behind the canines and molars in the back. The molars and incisors are used for chewing and it is speculated that once the molars lose their grinding effect due to wear the hippopotamus dies (Laws 1968). The canines appear to be used for defensive purposes and fighting for dominance. A photograph of a canine hippo tooth is shown in Figure 12(a). The tooth is curved and has a length of ~ 10 cm. A typical cross-section of the tooth is shown in Figure 12(b) (Espinoza and Mann, 1991). The structure is similar to other mammalian teeth, with dentin as the largest fraction surrounded by a thin layer or enamel or cementum. The interstitial zone is also known as the pulp cavity. The enamel of the hippo tooth has a density of 1.7 g/cm^3, had a compressive elastic modulus (enamel and dentin) of ~ 2.6 GPa and a hardness of 1.7 GPa for enamel and 0.3 GPa for dentin. This compares favorably with human teeth with a hardness of 3.2-4.4 GPa for enamel and 0.25-0.80 GPa for dentin (Marshall et al., 1997). The dentine-enamel interface has been shown to be an effective crack arrester. Cracks starting in the harder enamel are arrested at the interface (Imbeni et al. 2005).

Warthogs (*Phacochoerus Africa*) have two pairs of tusks on the lower and upper jaw. The tusks are the canine teeth, which continue growing during the life of the animal. The upper canines grow from 20-50 cm, while the lower ones grow to about 10 cm. The upper tusks (Figure 12(b)) grow out and curve up around the snout and are relatively dull. The lower tusks are short and straight and are used for defense and are kept self-sharpened due

to rubbing against the upper tusks. The tusks are sometimes used for digging but are generally used for fighting with other warthogs and for fending off predators. Fighting between warthogs for mating rights is usually done with a closed mouth where the warthogs face head to head and shove each other with the help of the dull upper tusks. On the other hand, warthogs will use their sharp lower tusks and an open mouth causing considerably more damage to fend off predators

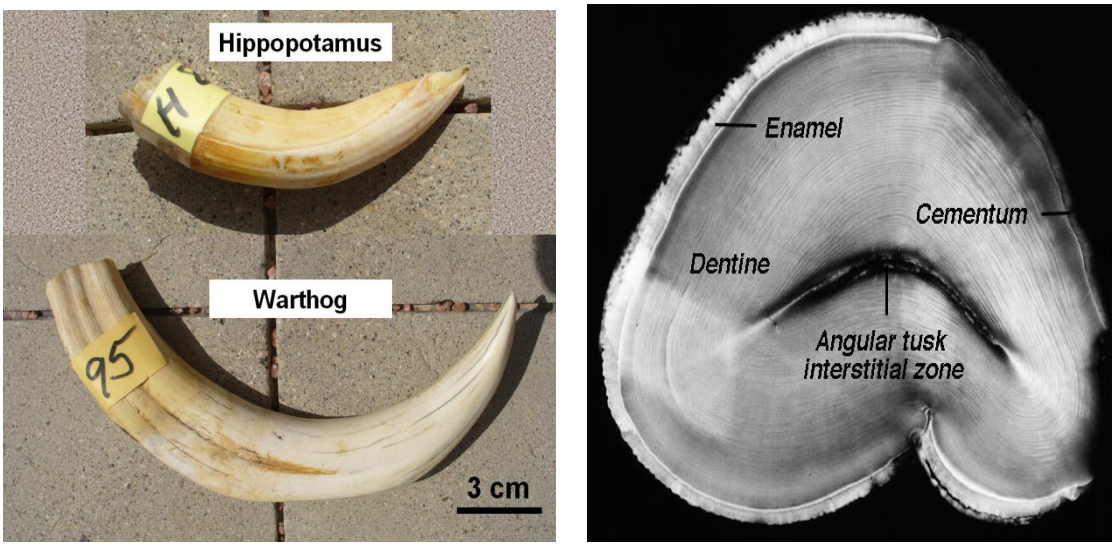

(a) **(b)**

Figure 12. (a) Photograph of the hippopotamus canine tooth and warthog tusk, (b) cross-section of the hippo tooth (Espinoza and Mann, 1991). (Tusks were purchased from Into the Wilderness Trading Company, Pinedale, WY. Teeth were obtained from piranha and the Amazon dogfish caught in Brazil.)

Figure 13 shows an SEM micrograph of a fracture surface of the dentin in the warthog tusk. The channels observed are the dentin tubules, which extend both from the enamel-dentin and cementum-dentin. The tubules contain fluid and cells and are surrounded by a highly mineralized layer and are

oriented perpendicular to the collagen fibrils in the dentin (Marshall et al., 1997). The tubule diameter (~ 1.3 µm) is on the order of what is reported for human dentin (~ 1.8 µm) direction, ranging between 12-45 MPa. This variability is most likely due to the difficulty in obtaining reliable test specimens from the curved tusk. (Marshall et al., 1997) and observed in elephant tusks (~ 1 µm) (Nalla et al., 2003). There was great variability in the tensile strength of the tusk in the longitudinal direction, ranging between 12-45 MPa. This variability is most likely due to the difficulty in obtaining reliable test specimens from the curved tusk.

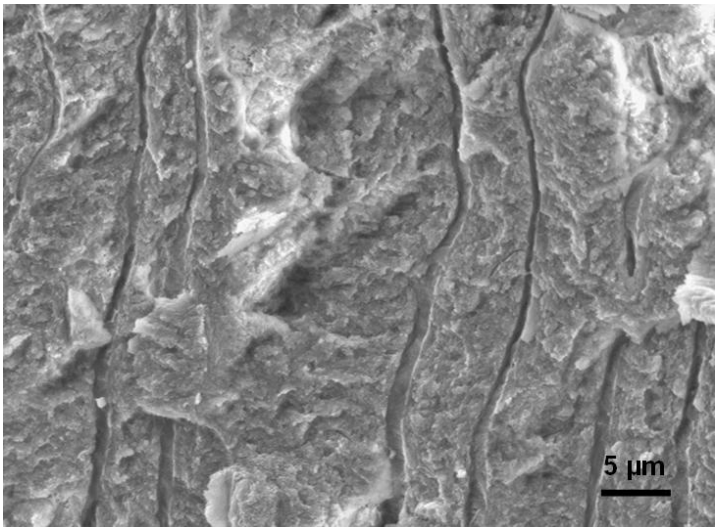

Figure 13. SEM micrograph of a fracture surface of a warthog tusk. The channels are the dentin tubules, which is surrounded by a collagen/mineral matrix.

One particularly important aspect of canine teeth is that the animal has the ability to sharpen their tip throughout its life. This has an obvious advantage for effective defense and hunting skills. This is accomplished in rodents and boars, and Figure 14 illustrates this effect. Figure 14(a) shows the incisor teeth in a rat. During eating, the dentine is eroded and results in a sharp enamel edge being continuously exposed.

This must be done continuously as these teeth keep growing during the life of the animal. Boars use the same approach to ensure a lethal cutting edge in the lower tusks. The area where wear is observed is marked in Figure 14(b), indicating this self-sharpening mechanism.

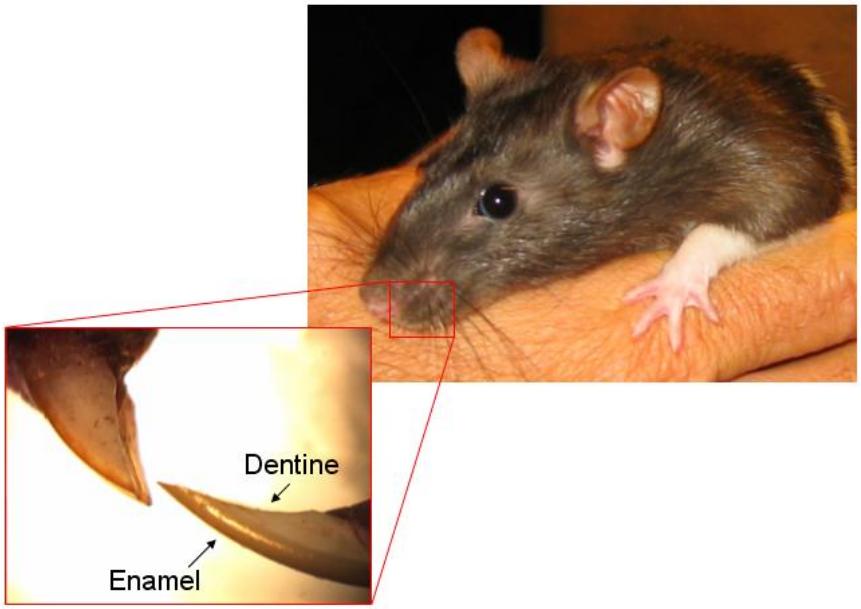

(a)

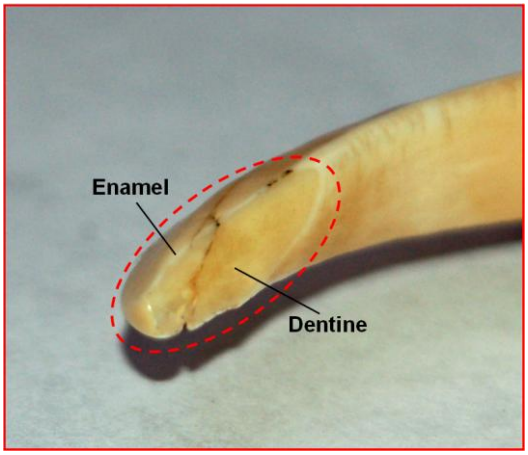

(b)

Figure 14. (a) Incisor in rat showing both the enamel and the dentine; (b) tusk in boar showing wear of dentine at tip, ensuring a sharp enamel edge. (Rat teeth were from a field rat.)

The Amazon dogfish (*Rhaphiodon vulpinus)* is a freshwater fish found in Central and South American river basins. It has two long teeth that penetrate through the mouth, as shown in Figure 15.

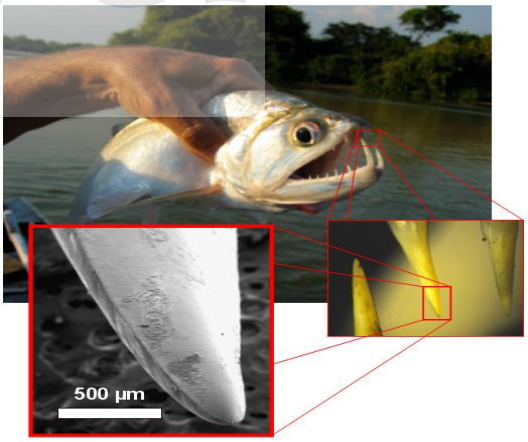

Figure 15. Dog fish and teeth. SEM images show the tooth to be sharp and pointed, but not serrated. (Teeth were obtained from piranha and the Amazon dogfish caught in Brazil.)

As shown in the SEM micrograph, the teeth are microstructurally smooth. The main function of these teeth is to puncture and hold prey rather than for slicing or sawing prey. Piranha (*Serrasalmus manueli*), on the other hand, has serrated teeth, as shown in the SEM micrographs in Figure 16. There are about 14 teeth on top and 12 on bottom in this fish. The lower teeth are longer and larger than the upper teeth. The large teeth are thin and leaf-like with serrated cutting edge along the entire tooth (Abler, 1992). The periodic distance of the serration is ~ 25 µm.

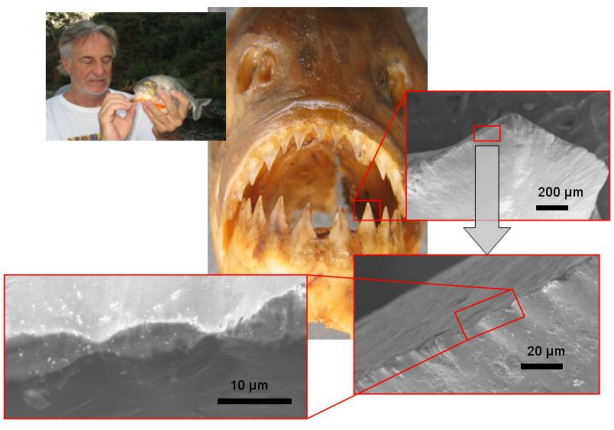

(a)

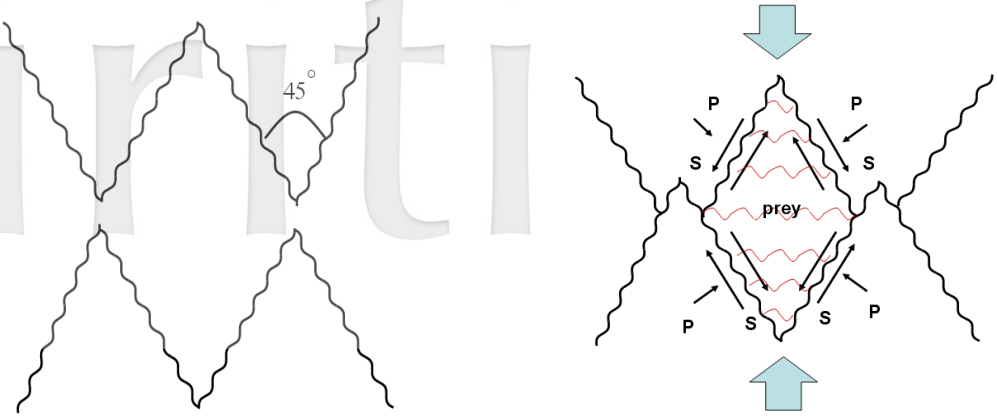

(b) **(c)**

Figure 16. Piranha Teeth: (a) hierarchical structure from jaw to single tooth to micro serrations; (b) and (c) Diagram of guillotine-like confinement of material during the biting action of a piranha. (Teeth were obtained from piranha and the Amazon dogfish caught in Brazil.)

The great white shark has five rows of wedge-shaped, triangular teeth in the upper (26) and lower jaw, as shown in Figure 17. These rows of teeth are fluid in the sense that the back teeth migrate to the front as the outermost, primary teeth are broken or torn off. The upper teeth are the slicing teeth and have obviously serration, as shown in the SEM micrographs. The serration has a periodic separation distance of ~ 300 μm, much larger than in the piranha teeth. The lower teeth have no serration and the difference is due functional reasons.

The sharp lower teeth, puncturing teeth are used to pierce the prey, however; the upper teeth are used to slice and cut the prey. Because of the serration, the biting force can be concentrated on each point, in comparison with the smooth-edge teeth, and thus have higher cutting efficiency. Other species of shark have differently shaped teeth such as knife-shaped or conical. For example, the sand tiger shark has a reverse curvature on the tip of their teeth, which ensures the initial penetration (Frazzetta, 1988). The inward curvature on the bottom of the lower teeth can hold the prey.

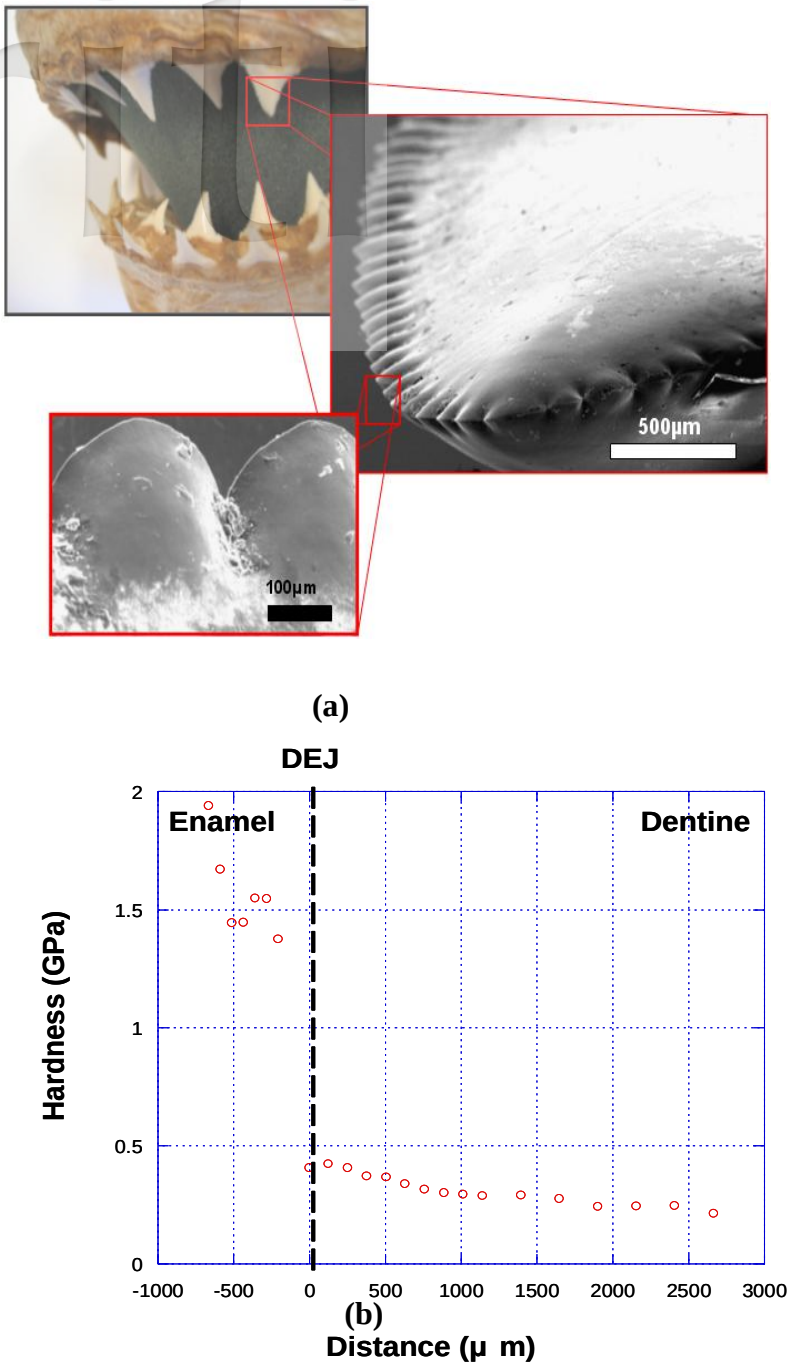

Figure 17. Great white shark teeth. (a) SEM images show serration at the edges of the tooth, (b) Hardness test showing DEJ junction. (Great white shark teeth were provided by Scripps Institute of Oceanography from their collection.)

The serration size appears to depend on the diet of the animal. Table I lists some carnivorous animals and a piscavore (piranha) with their body mass and serration size. Meat eaters, such as the tyrannosaurid dinosaurs, great white shark and komodo dragon have serration sizes ringing from 300 – 400 µm, despite having a two order of magnitude difference in body mass, as shown in Table I. Piranha, normally fish eaters,

has a much smaller serration size (~ 25 µm). From this, teeth seem to be optimized for tearing meat (large serrations) or for tearing fish (small serrations).

Table I. Teeth serration size and body mass for some carnivorous animals and the piranha.

	serration size (µm)	body mass (kg)	Ref.
Tyrannosauroid dinosaurs	312	6000	Abler, 1992
Great white shark	300	890	this work
Komodo dragon	400	70	Abler, 1992
Piranha	25	1	this work

CONCLUSION

Biological materials are adapted to be multifunctional. At the macroscale, the shape is generally optimized for protection and defense. At the microstructural scale, laminar, porous and fibrous structures predominate. Mineralized tissues provide protection and/or serve as a weapon and also impart a structural framework. Nacre, antlers, teeth and tusks have a hard, mineralized outer layer and a softer core. In nacre and enamel, the mineralized component is ~ 95%, far exceeding other mineralized components. The hard outer layer for abalone serves as protection whereas in teeth and tusks, it also provides biting and chewing surfaces. Teeth and tusks also function as defensive and offensive weapons. The shape of teeth is adapted for chewing (flat), piercing (sharp) or biting (sharp) whereas tusks are pointed and serve no function for nutritional purposes. The serrated teeth of predators such as sharks and piranha are additionally adapted to cutting. The softer inner core of teeth (dentin) provides toughness to the tooth with its woven, cross-laminar structure. For the crab exoskeletons, the mineralized portions protect and form a general framework for growth. Antlers, the horseshoe crab exoskeleton contain a porous substance in the core. For antlers it primarily provides stiffness and energy absorbance.

MATERIAL SOURCES

Abalone was harvested from the abalone tank located at the Scripps Institute of Oceanography, sheep crabs were obtained locally from a fish market, a horseshoe crab was collected on a beach in Long Island, NY, antlers and tusks were purchased from Into the

Wilderness Trading Company, Pinedale, WY. Teeth were obtained from piranha and the Amazon dogfish caught in Brazil. Great white shark teeth were provided by Scripps Institute of Oceanography from their collection. Rat teeth were from a field rat.

ACKNOWLEDGEMENTS

We gratefully acknowledge support from Professor Falko Kuester for the 3-D visualization**,** Jackie Corbeil for the computer tomography scans, Evelyn York for scanning electron microscopy, Paul Price and Damon Toroian for demineralizing the antler and Moopi for chasing down the rat. This research was funded by the National Science Foundation, Division of Materials Research, Biomaterials Program (Grant DMR 0510138).

REFERENCES

Abler, W. L., 1992. The serrated teeth of tyrannosaurid dinosaurs, and biting structures in other animals. Paleobiol., 18 [2], 161-183.

Ashby, M.F., 1989. On the engineering properties of materials, Acta metall., 37 [5] 1273-1293.

Addadi, L., Joester, D., Nudelman, F., Weiner, S., 2006. Mollusk shell formation: A source of new concepts for understanding biomineralization process. Chem. Eur. J. 12, 980-987.

Arzt, E., Gorb, S. & Spolenak, R., 2003. From micro to nano contacts in biological attachment devices. Proc. Natl Acad. Sci. USA 100, 10603-10606.

Autumn, K., Liang, Y.A., Hsieh, S.T., Zesch, W., Chan, W.P., Kenny, T.W., Fearing, R., Full, R.J., 2000. Adhesive force of a single gecko foot-hair. Nature 405, 681-685.

Barthelat, F., Li, C.M., Comi, C., Espinosa, H.D., 2006. Mechanical properties of nacre constituents and their impact on mechanical performance. J. Mater. Res. 21, 1977-1986.

Bertram, J.E.A., Gosline, J.M., 1987. Functional design of horse hoof keratin: The modulation of mechanical properties through hydration effects. J. Exp. Biol. 130, 121-136.

Bertram, J.E.A., Gosline, J.M., 1987. Functional design of horse hoof keratin: The modulation of mechanical properties through hydration effects. J. Exp. Biol. 130, 121-136.

Bevelander, G., Nakahara, H., 1970. An electron microscope study of the formation and structure of the periostracum of a gastropod, *Littorina littorca*. Calc. Tiss. Res. 5, 1-12.

Blob, R.W., LaBarbera, M., 2001. Correlates of variation in deer antler stiffness: age, mineral content, intra-antler location, habitat and phylogeny. Biol. J. Linn. Soc. 74, 113-120.

Blob, R.W., Snelgrove, J.M., 2006. Antler stiffness in moose (*Alces alces*): correlated evolution of bone function and material properties? J. Morph. 267, 1075-1086.

Bonser, R.H.C., 1995. Longitudinal variation in mechanical competence of bone along the avian humerus. J. Exp. Biol. 198, 209–212.

Bouligand, Y., 1972. Twisted fibrous arrangements in biological materials and cholesteric meso phases. Tissue Cell 4, 189-217.

Cartwright, J.H.E., Checa, A.G., 2007. The dynamics of nacre self-assembly. J. R. Soc. Inter. 4, 491-504.

Chapman, D.I., 1975. Antlers—bones of contention. Mamm. Rev., 5 [4] 121-172.

Chen, P.Y., Lin, A.Y.M., McKittrick, J.M., Meyers, M.A., 2007. Structure and mechanical properties of crab exoskeletons. Acta Biomater. Submitted.

Clutton-Brock, T.H., 1982. The function of antlers. Behaviour 79, 108-124.

Craig, R.G., Peyton F.A., Johnson, D.W., 1961. Compressive properties of enamel, dental cements and gold. J. Dent. Res. 40, 936-945.

Craig, R.G., Peyton F.A., 1958. Elastic and mechanical properties of human dentin. 37, 710-718.

Currey, J.D., 1979. Mechanical properties of bone tissues with greatly differing functions. J. Biomech. 12, 313-319.

Currey, J.D., 1988. The effect of porosity and mineral content on the Young's modulus of elasticity of compact bone. J. Biomech. 21, 131-139.

Currey, J.D., 1989. Strain rate dependence of the mechanical properties of reindeer antler and the cumulative damage model of bone fracture. J. Biomech. 22, 469-475.

Currey, J.D., 1990. Physical characteristics affecting the tensile failure properties of compact bone. J. Biomech. 23, 837-844.

Erben, H.K., 1972. On the structure and growth of the nacreous tablets in gastropods. Biomineral. 7, 14-27.

Espinoza, E.O., Mann, M.J., 1991. Identification guide for ivory and ivory substitutes. US Fish and Wildlife Services, Forensics Laboratory, Ashland, Oregon.

Falini, G., Albeck, G.S., Weiner, S., Addadi, L., 1996. Control of aragonite or calcite polymorphism by mollusk shell macromolecules. Science 271, 67-69.

Feng, Q.L., Li, H.B., Cui, F.Z., Li, H.D. Crystal orientation domains found in the single lamina in nacre of the *Mytilus edulis* shell. J. Mater. Sci. Lett. 18, 1547-1549.

Frazzetta, T.H., 1988. The Mechanics of cutting and the form of shark teeth (Chondrichthyes, Henshaw, Elasmobranchii). *Zoomorphology* 108, 93-107.

Fritz, M., Belcher, A.M., Radmacher, M., Walters, D.A., Hansma, P.K., Stucky, G.D., Morse, D.E., Mann, S., 1994. Flat pearls from biofabrication of organized composites on inorganic substrates. Nature 371, 49-51.

Gao, H.J., Ji, B.H., Jäger, I.L., Arzt, E., Fratzl, P., 2003. Materials become insensitive to flaws at nanoscale: lessons from nature. Proc. Natl. Acad. Sci. USA 100, 5597-5600.

Geist, V., 1966. The evolution of horn-like organs. Behaviour 27, 175-214.

Giraud-Guille, M.M., 1984. Fine structure of the chitin-protein system in the crab cuticle. Tissue Cell 16, 75-92.

Goss, R.J., 1983. Deer antlers: regeneration, function and evolution. Academic Press, New York.

Harvey, P.H., Bradbury, J.W., 1991. Sexual selection, in: Krebs, J.R. Davies, N.B. (Eds.), Behavioural ecology: an evolutionary approach. Blackwell Scientific, Oxford, pp. 203-233.

Henshaw, J., 1971. Antlers—the unbrittle bones of contention. Nature 231, 469.

Imbeni, V, Nalla, R.K, Bosi, C., 2003. In vitro fracture toughness of human dentin. J. Biomed. Mater. Res. A 66, 1-9.

Imbeni, V., Nalla, R.K., Marshall, G.W., Marshall, S.J., Ritchie, R.O., 2005. The dentin–enamel junction and the fracture of human teeth. Nature Mater. 4**,** 229-232.

Jackson, A.P., Vincent, J.F.V., Turner, R.M., 1988a. The mechanical design of nacre. Proc. Royal Soc. Lond. B 234, 415-440.

Jackson, A.P., Vincent, J.F.V., Turner, R.M., 1988b. Comparison of nacre and other ceramic composites. Proc. Royal Soc. Lond. B 234, 415.

Ji, B.H., Gao, H.J., 2004. Mechanical properties of nanostructure of biological materials. J. Mech. Phy. Solid 52,1963-1990.

Kitchener, A., Vincent, J.F.V., 1987. Composite theory and the effect of water on the stiffness of horn. J. Mater. Sci. 22, 1385-1389.

Laws, R.M., 1968. Dentition and aging of the hippopotamus. East African Wildlife Journal 6, 19-52.

Léonard, A., Guiot, L.P., Pirard, J.P., Crine, M., Balligand, M., Blacher, S., 2007. Non-destructive characterization of deer (*Cervus elaphus*) antlers by X-ray microtomography coupled with image analysis. J. Micros. 225, 258-263.

Lin, A.Y.M., Meyers, M.A., 2005. Growth and structure in abalone shell. Mater. Sci. Eng. A 290, 27-41.

Lin, A.Y.M., Meyers, M.A., Vecchio, K.S., 2006. Mechanical properties and structure of *Strombus gigas*, *Tridacna gigas* and *Haliotis rufescens* sea shells: a comparative study. Mater. Sci. Eng. C 26, 1380-1389.

Lin, A.Y.M., Chen, P.Y., Meyers, M.A., 2007. The growth of nacre in the abalone shell. Acta Biomater. In press.

Lincoln, G.A., 1972. The role of antlers in the behavior of red deer. J. Exp. Zool. 182, 233-249.

Lorensen, W.E., Cline, H.E., 1987. Marching cubes: A high resolution 3D surface construction algorithm. Comp. Graph. 21, 163-169.

Manne, S., Zaremba, C.M., Giles, R., Huggins, L., Walters, D.A., Belcher, A.M., Morse, D.E., Stucky, G.D., Didymus J.M., Mann, S., Hansma, P.K., 1994. Atomic force microscopy of the nacreous layer in mollusc shells. Proc. Royal Soc. B 236, 17-23.

Marshall, G.W., Marshall, S.J., Kinney, J.H., Balooch, M., 1997. The dentin substrate: structure and properties related to bonding. J. Dent. 25, 441-458.

Meister, W., 1956. Changes in biological structure of the long bones of white-tailed deer during the growth of antlers. Anat. Rec. 124, 709-721.

Menig, R., Meyers, M.H., Meyers, M.A., Vecchio, K.S., 2000. Quasi-static and dynamic mechanical response of *Haliotis rufescens* (abalone) shells. Acta. Mater. 48, 2383-2398.

Meyers, M.A., Chen, P.Y., Lin, A.Y.M., Seki, Y., 2007. Biological materials: Structure and mechanical properties. Prog. in Mater. Sci. In press.

Meyers, M.A., Lin, A.Y.M., Chen, P.Y., Muyco, J., 2008. Mechanical strength of abalone nacre: role of the soft organic layer. J. Mech. Behav. Biomed. Mater. 1, 76-85.

Muir, P.D., Sykes, A.R., Barrell, G.K., 1987. Calcium metabolism in red deer (*Cervus elaphus*) offered herbages during antlerogenesis: kinetic and stable balance studies. *J. Agric. Sci. Camb.* 109, 357-364.

Nakahara, H., Bevelander, G., Kakei, M., 1982. Electron microscopic and amino acid studies on the outer and inner shell layers of *Haliotis rufescens*. Venus Jpn. J. Malac. 41, 33-46.

Nalla, R.K., Kinney, J.H., Ritchie, R.O., 2003. Effect of orientation on the in vitro fracture toughness of dentin: the role of toughening mechanisms. Biomaterials 24, 3955-3968.

Raabe, D., Sachs, C., Romano, P., 2005. The crustacean exoskeleton as an example of a structurally and mechanically graded biological nanocomposite material. Acta. Mater. 53, 4281-4292

Rajaram, A., Ramanathan, N., 1982. Tensile properties of antler bone. Calc. Tiss. Int. 34, 301-305.

Sarikaya, M., Aksay, I.A., 1992. Nacre of abalone shell: a natural multifunctional nanolaminated ceramic-polymer composite material, in: Case, S.T. (Ed.), Results and Problems in Cell Differentiation –Biopolymers. Springer-Verlag, Berlin, pp. 1-26.

Schäffer, T.E., Zanetti, C.I., Proksch, R., Fritz, M., Walters, D.A., Almqvist, N., Zaremba, C.M., Morse, D.E., Hansma, P.K., 1997. Does abalone nacre form by heteroepitaxial nucleation or by growth through mineral bridges? Chem. Mater. 9, 1731-1740.

Seki, Y., Schneider, M.S., Meyers, M.A., 2005. Structure and mechanical properties of the toucan beak. Acta Mater. 53, 5281-5296.

Seki, Y., Kad, B., Benson, D., Meyers, M.A., 2006. The toucan beak: Structure and mechanical response. Mater. Sci. and Eng. C 26, 1412-1420.

Snodgrass, S.M., Gilbert, P.W., 1967. A shark bite meter, in: Gilbert, P.W., Mathewson, R.F., Rall, D.P. (Eds.), Sharks, Skates and Rays. The Johns Hopkins University Press, Baltimore, pp. 331-337.

Song, F., Zhang, X.H., Bai, Y.L., 2002. Microstructure and characteristics in the organic matrix layers of nacre. J. Mater. Res. 17, 1567-1570.

Srinivasan, A.V., Haritos, G.K., Hedberg, F.L., 1991. Biomimetics: Advancing man-made materials through guidance from nature. Appl. Mech. Rev. 44, 463-482.

Taylor, A.M., Bonser, R.H.C., Farrent, J.W., 2007. The influence of hydration on the tensile and compressive properties of avian keratinous tissues. J. Mater. Sci. 39, 939– 942.

Towe, K.M., Hamilton, G.H., 1968. Ultrastructure and inferred calcification of the mature and developing nacre in bivalve mollusks. Calc. Tiss. Res. 1, 306-318.

van der Lang, N.J., A.J.M. van Dijk, L.H.M.G. Dortmans and G. de With, 2002. Fracture toughness of calcium hydroxyapatite and spinel at different humidities and loading rates. Key Eng. Mater., 206-213, 1599-1602.

Vincent, J.F.V., 1991. Structure Biomaterials. Princeton University Press, New Jersey.

Vincent, J.F.V., 2002. Arthropod cuticle: a natural composite shell system. Composites A 33, 1311-1315.

Vollrath, F., Madsen, B., Shao, Z., 2001. The effect of spinning conditions on the mechanics of a spider's dragline silk. Proc. Royal Soc. B 268, 2339-2346.

Wada, K., 1964. Studies on the mineralization of calcified tissues in molluscs – VIII. Behavior of eosinophil granules and of organic crystals in the process of mineralization of secreted organic matrices in glass coverslip preparations. Nat. Pearl Res. Lab. 9, 1087-1098.

Watanabe, N., Wilber, K.M., 1960. Influence of the organic matrix on crystal type in mollusks. Nature 188, 334.

West, U.G.K., Ashby, M.F., 1994. The mechanical efficiency of natural materials. Philos. Mag. 84, 2167-2186.

Wu, K.S., van Osdol, W.W., Dauskardt, R.H., 2006. Mechanical properties of human stratum corneum: Effects of temperature, hydration, and chemical treatment. Biomaterials 27, 785-795.

Zaremba, C.M., Belcher, A.M., Fritz, M., Li, Y., Mann, S., Hansma, P.K., Morse, D.E., Stucky, G.D., 1996. Critical transitions in the biofabrication of abalone shells and flat pearls. Chem. Mater. 8, 679-690.

若干精選生物材料的結構、功能與力學性質

P.-Y. Chen[1], A.Y.M. Lin[1], Y.-S. Lin[2], M.A. Meyers[1,2] and J. McKittrick[1,2],
[1]Materials Science and Engineering Program, [2]Dept. of Mechanical and Aerospace Engineering, UC San Diego, La Jolla, CA 92037-0411

摘要

礦石化的生物組織讓我們得以知曉，大自然是如何讓這些成分進化、以達成多項功能最佳化的目的。這些礦物成分本身含量極微，然而與有機環境交互作用的結果造就其擁有超乎尋常力學特性的材料。這些材料的總合結構是此一增強的關鍵所在。像是有機、層狀有/無機結構的微結構特徵，還有孔狀和纖維狀要素的存在，這些在許多生物的構成上都是常見的。有機與無機部分在分子級與微層級協同作用的結果、增強了力學功能。在本論文中，我們就近來關於鮑魚殼、螃蟹殼、鹿角、獠牙、牙齒的進展提出報告。

關鍵字：力學性質；生物材料；仿生學；鮑魚；蟹；鱟；鹿角；河馬牙；非洲野豬獠牙；大白鯊牙；淡水虎魚牙；狗魚牙

收文日期：99 年 09 月 15 日　接受日期：99 年 09 月 23 日

通訊作者及聯絡地址：陳柏宇，美國加州大學聖地牙哥分校(UCSD)材料博士，9500 Gilman Drive, La Jolla, CA 92093-0411
E-mail：pochen@ucsd.edu